Transportation Science

Publication details, including instructions for authors and subscription information:
http://pubsonline.informs.org

Analysis and Design of Rack-Climbing Robotic Storage and Retrieval Systems

Wanying Chen, René De Koster, Yeming Gong

To cite this article:
Wanying Chen, René De Koster, Yeming Gong (2022) Analysis and Design of Rack-Climbing Robotic Storage and Retrieval Systems. Transportation Science 56(6):1658-1676. https://doi.org/10.1287/trsc.2022.1140

https://pubsonline.informs.org/journal/trsc

TRANSPORTATION SCIENCE
Vol. 56, No. 6, November–December 2022, pp. 1658–1676
ISSN 0041-1655 (print), ISSN 1526-5447 (online)

Analysis and Design of Rack-Climbing Robotic Storage and Retrieval Systems

Wanying Chen,[a] René De Koster,[b] Yeming Gong[c,*]

[a] School of Management and e-Business, Zhejiang Gongshang University, Hangzhou 30018, China; [b] Rotterdam School of Management, Erasmus University, 3062PA Rotterdam, Netherlands; [c] Emlyon Business School, 69130 Ecully, France
*Corresponding author

Contact: wanyingchen@mail.zjgsu.edu.cn, https://orcid.org/0000-0002-8650-4888 (WC); rkoster@rsm.nl, https://orcid.org/0000-0002-1740-7822 (RDK); GONG@em-lyon.com, https://orcid.org/0000-0001-9270-5507 (YG)

Received: October 6, 2020
Revised: April 17, 2021; September 27, 2021; January 12, 2022; February 5, 2022
Accepted: February 12, 2022
Published Online in Articles in Advance: April 7, 2022

https://doi.org/10.1287/trsc.2022.1140

Abstract. Warehouses are becoming increasingly robotized. Autonomous rack-climbing robots have recently been introduced in e-commerce fulfillment centers. The robots not only retrieve loads from any level in a rack but also, roam the warehouse and bring the loads to order picking stations without using conveyors or lifts. This paper models and analyzes this system under both single and dual commands with different robot assignment (dedicated versus shared) and storage location assignment (class-based and random) policies. We study these policies in the presence of robot congestion. We evaluate the impact of two blocking protocols, a wait-outside-aisle policy and a block-and-recirculate policy, on the order throughput time. The system is modeled using semiopen queuing networks (SOQNs) for the different operating policies. The analytical models are validated using simulation. We also use this model to compare this system with a shuttle-based system. The results show that (1) the choice of the wait-outside-aisle policy or the block-and-recirculate policy mainly depends on the number of the robots in the system and the throughput requirement and that (2) the dedicated robot assignment policy can be an attractive policy, especially for a large system.

Funding: W. Chen was supported by the National Natural Science Foundation of China [Grant 72001189] and Qianjiang River Talent Scholarship [Grant QJC1802002]. Y. Gong is supported by the Artificial Intelligence in Management Institute and Business Intelligence Center.
Supplemental Material: The online appendix is available at https://doi.org/10.1287/trsc.2022.1140.

Keywords: warehousing • facility logistics • robot • queueing networks • blocking • assignment policy • storage policy

1. Introduction

Our research is motivated by new robotic storage and retrieval systems that use rack-climbing robots. A rack-climbing robotic storage and retrieval (CRSR) system can use robots to move unit loads in three dimensions. A CRSR system includes three main parts: aisles that include single-deep storage racks, a remotely located workstation where products are picked for customer orders from totes, and robots that can climb the racks to collect totes and transport totes between aisles and the workstation at the ground floor. In this system, each aisle contains two single-deep storage racks with vertical-direction rails in each rack section. The robots can use these rails to climb and descend in each rack section. All horizontal movements are carried out at the ground level. One such system has been developed by a French company Exotec and has several implementations in firms such as C-discount, E.LECLERC, and Carrefour (Exotec Solutions 2019). Attabotics is another supplier of such systems (Attabotics 2020a, b).

Different shuttle or autonomous mobile robotic (AMR) systems (for more information about AMR systems, see Azadeh, Roy, and De Koster 2019b) can be distinguished (e.g., the autonomous vehicle-based storage and retrieval (AVS/R) systems (Malmborg 2002, Kuo, Krishnamurthy, and Malmborg 2007, Tappia et al. 2016), puzzle-based compact storage and retrieval (PCS/R) systems (Gue and Kim 2007), the vertical AVS/R systems (Azadeh, Roy, and De Koster 2019a), and the robotic mobile fulfilment (RMF) systems (Yuan and Gong 2017, Weidinger, Boysen, and Briskorn 2018, Lamballais, Roy, and De Koster 2020)). Compared with these systems, the robot in a CRSR system can freely roam on the ground floor between the aisles in addition to climbing vertically in the rack. This makes the CRSR system flexible and scalable.

Our paper investigates the analysis and design of a CRSR system. The order throughput time is a key performance measure, as it indicates the duration to finish an order; also, it reflects the service offered by the CRSR system. Different factors (e.g., the layout of the system, the blocking delays of robots) may impact the order throughput time. A particular challenge is to determine the assignment of robots to aisles. Because the robots can move between different aisles, the assignment of robots to aisles affects the order throughput time. In

this paper, we study the dedicated assignment and the shared assignment. In a dedicated assignment, each aisle has dedicated robots to store or retrieve the totes. In a shared assignment, all aisles share all robots. Increasing the quantities of robots may cause robot blocking and congestion. However, more robots can decrease the order throughput time. We consider two blocking policies to mitigate this problem, a block-and-recirculate (BAR) policy (see Azadeh, Roy, and De Koster 2019a) and a wait-outside-aisle (WOA) policy. We also consider two storage policies: class-based storage, based on a decision of the storage space in time turnover frequency classes, and random storage.

In this paper, we investigate the following main research questions.

1. How do we establish analytical models to estimate the order throughput time of the CRSR system considering these operating policies?
2. Which blocking policy, a block-and-recirculate policy or a wait-outside-aisle policy, leads to shorter order throughput time for a given number of robots?
3. Which assignment policy is best: dedicated or shared?
4. What rack structure (length and height) is the most beneficial for a CRSR system while taking robot blocking into account?

To answer the research questions, we study the system using semiopen queuing networks (SOQNs), which can handle these operating policies and synchronize orders with robots. The system with the block-and-recirculate policy is modeled as an SOQN with finite capacity nodes. We use mean value analysis for jump-over networks to calculate the order throughput time under the block-and-recirculate policy and adopt an aggregation method to estimate the order throughput time under the wait-outside-aisle policy. We then use simulation to validate our models. Analytical models are used to study the assignment policy of robots to aisles and to compare different assignment policies. We also compare the wait-outside-aisle and block-and-recirculate policies and investigate the effect of blocking delays.

Our paper has the following contributions. (1) We develop accurate analytic models to estimate system performance for these new rack-climbing robotic storage and retrieval systems. (2) We contribute system design insights. We investigate the optimal rack size of this new system and compare two assignment policies in the presence of robot congestion. We also compare two blocking policies on the system performance. We compare cost and system performance of the rack-climbing robotic storage and retrieval system with traditional AVS/R systems with external workstations. This comparison can be found in Online Appendix F.

We organize the remainder of the paper as follows. We review the related papers in Section 2. The system and the operating polices are presented in Section 3. The analytical models are shown in Section 4. Section 5 presents solution approaches. In Numerical results are presented in Section 6. Section 7 draws conclusions and suggests future works.

2. Literature Review

This section reviews the literature on shuttle or AMR systems and on queueing networks with the block-and-recirculate protocol.

2.1. Shuttle or AMR Systems

Shuttle or AMR systems can be distinguished in different types, such as the PCS/R system (Gue and Kim 2007), the AVS/R system (Malmborg 2002, Kuo, Krishnamurthy, and Malmborg 2007, Tappia et al. 2016), the vertical AVS/R system (Azadeh, Roy, and De Koster 2019a), and the RMF system (Yuan and Gong 2017, Weidinger, Boysen, and Briskorn 2018, Merschformann et al. 2019, Lamballais, Roy, and De Koster 2020).

In a PCS/R system, all loads (e.g., pallets or totes containing the stock keeping units (SKUs)) are stored on semiautonomous shuttles (or conveyor modules), which can transport them from and to a depot. All loads are stored in a grid, which has only a few open locations (called "escorts") to achieve a very high storage density. The system moves the open locations repeatedly, like in a Sam Loyd's puzzle game, to create a retrieval path for the requested load to the depot. This application is currently used in automated parking systems, whereas applications in warehouses are mostly in a pilot stage. Gue and Kim (2007) study a single tier of the PCS/R system and obtain closed-form results of retrieval time. Zaerpour, Yu, and De Koster (2017b) investigate a multitier PCS/R system and derive closed-form expressions for the expected retrieval time. They propose a mixed integer nonlinear model to optimize the system dimensions. Zaerpour, Yu, and De Koster (2017a) study the class-based storage policy in a PCS/R system. They conclude that their proposed storage policy can improve the average response time of the system up to 55% compared with the random storage policy.

AVS/R systems were introduced by Savoye Logistics in the 1990s. A typical AVS/R system is aisle based. Semiautonomous vehicles (shuttles) drive on rails and store and retrieve totes at the different tiers, whereas lifts take care of the vertical tote transport. The number of lifts may constrain the throughput capacity. Such systems have high throughput capacity because of the large number of shuttles and are frequently used in e-commerce warehouses to handle small items with medium turnover speed. Different types of queuing network models have been used to estimate the performance of AVS/R systems (e.g., open queueing networks (Heragu et al. 2011, Marchet

et al. 2012, Epp, Wiedemann, and Furmans 2016), semiopen queueing networks (Roy et al. 2012, 2015, 2017; Cai, Heragu, and Liu 2014; Tappia et al. 2016), fork-join queueing networks (Zou et al. 2016), nested queueing networks (Kuo, Krishnamurthy, and Malmborg 2007, Fukunari and Malmborg 2008), and closed queueing networks (Fukunari and Malmborg 2008)). Heragu et al. (2011), Marchet et al. (2012), and Epp, Wiedemann, and Furmans (2016) evaluate the transaction cycle time of the tier-captive AVS/R system by the open queueing network. In order to study how the number of vehicles impacts the system performance, some researchers adopt SOQN because SOQN can give an accurate representation of the system when the transport vehicle is a common constrained resource that should be used by all jobs. Cai, Heragu, and Liu (2014) and Ekren et al. (2014) build an SOQN to study an AVS/R system with tier-to-tier vehicles. Roy et al. (2015) use SOQN to study how the dwell point of vehicles and the location of a crossaisle affect the system performance. Zou et al. (2016) study the parallel operation of the AVS/R system by a fork-join queueing network. Kuo, Krishnamurthy, and Malmborg (2007) and Fukunari and Malmborg (2008) study the AVS/R system by a nested queueing network model. Malmborg (2002) uses continuous Markov chain models to study the vehicle utilization and expected response time.

A vertical AVS/R system is similar to an AVS/R system, but it does not contain lifts. Robots are aisle captive and climb the rack in the first column; then, they travel at the top tier to the designated column, descend, and retrieve or store a tote at the designated position. They then travel to the bottom tier and move to the pick station located at the aisle end. Azadeh, Roy, and De Koster (2019a) study a vertical AVS/R system with a single aisle using a closed queuing network (CQN). They optimize the shape of the rack and study how different robot blocking policies impact the system performance.

The RMF system consists of movable "pods" (a storage shelf) containing products and robots, which can drive underneath the pods to fetch them and transport them to workstations, where items can be picked or replenished. The literature about the RMF system focuses on design optimization and operational control. Lamballais, Roy, and De Koster (2020) show that the location of workstations impacts the maximum order throughput. Zou et al. (2017) adopt an SOQN to optimize the shape of the system. Yuan and Gong (2017) develop an SOQN to calculate the optimal number of the robots to achieve a certain throughput time. Zou et al. (2018) propose an SOQN to investigate different battery recovery strategies for the RMF system. Merschformann et al. (2019) develop simulation models to study various decision problems, including the order to station assignment, pod selection, and pod storage assignment choices. Roy et al. (2019) analyze both order picking and replenishment processes in an RMF system based on multiclass CQN.

A CRSR system combines elements of RMF systems as the robots can freely roam between different aisles horizontally, on the ground, to transport totes between the aisles and a workstation. It also has elements of the vertical AVS/R systems because the robots can climb and descend in a rack section. However, it also differs from these systems. Unlike the vertical AVS/R systems, the robots move on the ground before climbing, and they can freely roam between aisles and the workstation, which gives them higher flexibility in deployment.

2.2. Queueing Networks with the Block-and-Recirculate Protocol

This paper uses two different protocols to reduce the congestions to prevent blocking. Antiblocking protocols have been studied in both manufacturing and warehouse environments. Papadopoulos and Heavey (1996), Perros (1994), and Balsamo et al. (2001) review queueing networks with blocking in the manufacturing environment. Yao and Buzacott (1987) study flexible manufacturing systems with a variation of the block-and-recirculate protocol in warehouses. Van der Gaast et al. (2020) develop a capacity model for sequential zone picking systems using the block-and-recirculate protocol. The systems are modeled as a multiclass block-and-recirculate closed queueing network. Azadeh, Roy, and De Koster (2019a) use these results and build a closed queueing network with the block-and-recirculate protocol for the vertical AVS/R system with a recirculation blocking policy. They present a jump-over approximation method to estimate the performance of the system. Tappia et al. (2019) use a CQN to study the blocking delays in integrated storage-order picking systems with block-and-recirculate protocol. A jump-over method is used to solve the CQN proposed in Tappia et al. (2019).

Table 1 summarizes the differences among the systems studied in this paper and the systems investigated in the literature. Our system is close to the vertical AVS/R system studied by Azadeh, Roy, and De Koster (2019a). It differs from the vertical AVS/R system because the vehicles can roam the aisles. This makes it necessary to study the effect of the robot-to-aisle assignment in combination with robot blocking and congestion.

3. System Description

The CRSR system is described in Section 3.1. Section 3.2 describes the robots assignment policies studied in this paper. Section 3.3 discusses the blocking policies.

3.1. Rack-Climbing Robotic Storage and Retrieval Systems

Figure 1 illustrates the layout of a CRSR system. It includes three components: aisles with single-deep

Table 1. Overview of Main Literature

System features	Reference	Blocking delay	Robot-aisle assignment
AVS/R: Horizontal movements by aisle-captive vehicles; vertical movements by lifts; high-level storage racks	Malmborg (2002),; Kuo, Krishnamurthy, and Malmborg (2007); Fukunari and Malmborg (2008); Marchet et al. (2012); Roy et al. (2014, 2015, 2016, 2017); Zou et al. (2016)	None; collision-avoidance protocol	Shared; shared
Vertical AVS/R: Horizontal and vertical movements by aisle-captive robots; high-level storage racks	Azadeh, Roy, and De Koster (2019a)	Wait-on-spot; block-and-recirculation policies	Shared
RMF: Horizontal movements by robots; low-level mobile racks	Yuan and Gong (2017); Zou et al. (2017); Merschformann et al. (2019); Roy et al. (2019); Lamballais, Roy, and De Koster (2020)	None	Shared; robots assigned to storage zones
PCS/R: Horizontal movements by shuttles; vertical movements by lifts; compact storage without aisles	Gue and Kim (2007); Zaerpour, Yu, and De Koster (2017a, b)	None	Shared
CRSR: Horizontal and vertical movements by rack-climbing robots; high-level storage racks	This paper	Wait-outside-aisle, block-and-recirculate policies	Dedicated and shared assignment policies

storage racks, a remotely located workstation, and robots that can climb the racks and transport stored product totes between aisles and the workstation. The workstation is located at the bottom center. The products are stored in high-level racks and brought to the workstation by rack-climbing robots. The robots can independently transport totes between storage locations and the workstation at the ground floor and climb the storage rack to retrieve or store totes. When a retrieval transaction is completed, the robot dwells at the workstation. Traffic in the aisles and crossaisles is unidirectional. A side view of the CRSR system with a single aisle is shown in Figure 2. Each robot can climb and descend vertically in a rack section and access each storage position within the aisle by moving horizontally on the ground floor. We shows the main notations in Table 2.

Following the allowed direction, the control system assigns the robot from its dwell point to the designated location. Because in practice, both single and dual commands are applied (Exotec Solutions 2019), in the remainder of the paper, we investigate both dual commands (storage followed by a retrieval) and single commands (retrieval transaction only). We assume that orders arrive according to a Poisson process. This is a reasonable assumption for online order arrivals. It is, however, possible to model other (e.g., phase-type) distributions in an approximate fashion, albeit at the expense of a more complex analysis and possible loss of accuracy. The operational steps are as follows.

a. If a robot is not available, the arriving order must wait in the first come, first served sequence; otherwise, an available robot will be assigned to handle the order, and the robot moves from its workstation (dwell point) to the entrance of designated aisle i, following the allowed travel direction (μ_i^a).

b. The robot moves from the aisle entrance to the bottom of the designated rack section. For the single-command cycle, the robot climbs to the retrieval position, loads the tote, and descends to the bottom of rack. For a dual-command cycle, the robot climbs to the storage position, unloads the tote, descends to the bottom of the storage rack, moves to the designated rack for the retrieval, climbs to the retrieval position, loads the tote, and descends to the bottom of rack (μ_b).

c. The robot moves from the exit of the aisle i to the workstation, following the allowed travel direction (μ_i^c).

d. If the worker is not available, the robot waits for service at the workstation. Otherwise, the worker handles the robot at the workstation (μ_w).

The storage location assignment policy influences performance. We have selected two dominant rules from practice: random and class-based storage. Random assignment is frequently used, as demand is often unknown or nonstationary. Class-based storage is robust against demand fluctuations and optimal for a small number of classes when taking space consumption of multiple loads per product into account, according to Yu, De Koster, and Guo (2015). However, other choices are possible (e.g., the "linear decision

Figure 1. Top View of a CRSR System

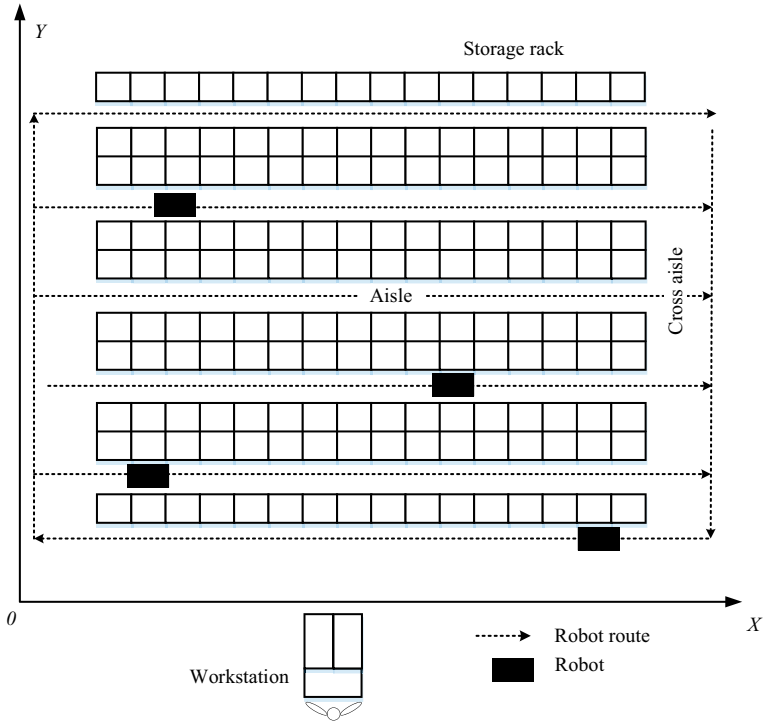

rule") (Ang, Lim, and Sim 2012, Ang and Lim 2019), which may impact the system performance.

Under the random storage policy, all products are stored randomly over the aisles and locations. Under the class-based storage policy, products are classified into a small number (typical three) of classes according to their turnover. The storage positions are also divided into the same number of areas (see Online Appendix A). Because the robot travel time is the sum of vertical travel time (depending on distance from the ground level) and horizontal travel time (constant for a given aisle), the optimal item allocation division, minimizing the total travel time, will be along horizontal tiers, as in this way, the fast movers can be given a shorter total travel time compared with an allocation in groups of rack sections. The highest-turnover product class, containing N_{sp}^{A} products, is assigned to the lowest n_A rack tiers. Products from the lowest-turnover class

Figure 2. Robot Blocking (Aisle Side View with Maximum Four Robots in Each Aisle)

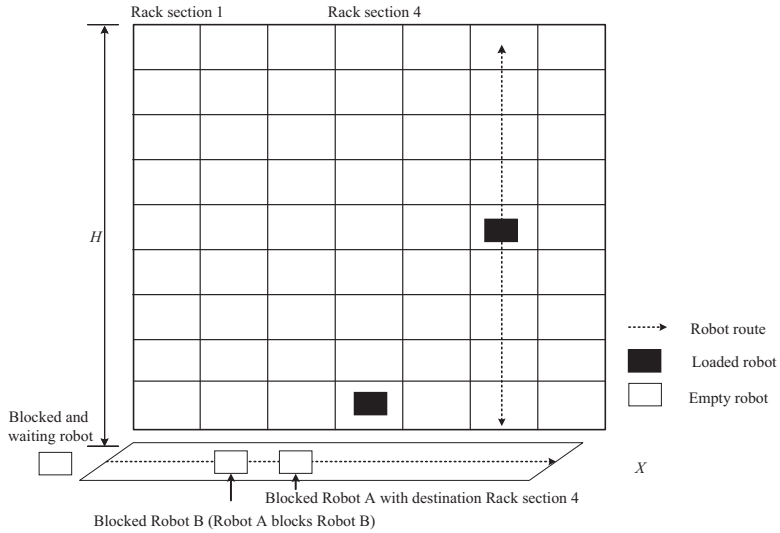

Table 2. The Notations Used in This Paper

Notation	Description
w, l, h	Width, length, and height of a storage position (m)
n_l, n_h	The number of rack sections and tiers in one shelf rack (system length and height)
n_a	The number of aisles
w_a, w_c	Width of an aisle and crossaisle (m)
C	System storage capacity, $C = 2n_a n_l n_h$
C_o	Storage positions in one rack, $C_o = n_l n_h$
N	The number of robots in the system
v_v, v_h	The velocity of robots in the vertical direction and on the ground, respectively (m/s)
t	The load/unload time of a robot (s)
D_{a_i}	The travel distance between the workstation and the entrance of the aisle i (m)
λ	The order arrival rate (per hour)
N_{sp}	The number of storage position in each storage rack
F_A, F_B, F_C	Demand rate of products belonging to the storage zone A, B, or C
N_{sp}^k	The number of storage positions in tier k, $k = 1, 2, \ldots, n_h$
K	Ratio of ordering cost to holding cost rate in each storage rack
n_A, n_B, n_C	Height of A, B, C zones in each storage rack (by the number of tiers)
P_A, P_B, P_C	Probability that the product belongs to A, B, C class in each storage rack
T_i^a	The travel time from the workstation to the entrance of the aisle i, $i = 1, 2, \cdots n_a$ (s)
T_b	The service time in the aisle (s)
T_i^e	The travel time from the exit of the aisle i to the workstation(s)
$T_{e_i,w}$	The travel time from the exit of the aisle i to the workstation, $i = 1, 2, \cdots n_a$ (s)
P_i^a	The routing probability of a robot to aisle i in the shared assignment policy, $i = 1, 2, \cdots n_a$
p_i^b	The blocking probability at aisle i, $i = 1, 2, \cdots n_l$
t_w	The handling time at the workstation (s)

(N_{sp}^C products in total) are stored in the n_C-highest tiers in the rack. The remaining N_{sp}^B products are stored in the intermediate n_B levels of the rack.

Equation (1) calculates the number of storage positions demanded by every product class:

$$N_{sp}^A = \sum_{k=1}^{n_A} N_{sp}^k, \quad N_{sp}^B = \sum_{k=n_A+1}^{n_A+n_B} N_{sp}^k, \quad N_{sp}^C = \sum_{k=n_A+n_B+1}^{n_h} N_{sp}^k. \tag{1}$$

Therefore, for a given demand curve and number of products per storage class, the number of storage positions in one storage rack is $N_{sp} = N_{sp}^A + N_{sp}^B + N_{sp}^C$. The height-to-length ratio of the shelf rack is $r = n_h/n_l$. Assuming a continuous space storage rack, we can obtain the length and height rack by Equation (2):

$$n_l = (N_{sp}/r)^{1/2}, \quad n_h = r n_l. \tag{2}$$

Moreover, we can obtain the height of each zone area by Equation (3):

$$n_A = \frac{n_h N_{sp}^A}{N_{sp}}, \quad n_B = \frac{n_h N_{sp}^B}{N_{sp}}, \quad n_C = \frac{n_h N_{sp}^C}{N_{sp}}, \tag{3}$$

where $n_A + n_B + n_C = n_h$.

3.2. Assignment Policies of Robots to Aisles

In a CRSR system, the rack-climbing robots can move between different aisles. We investigate two robot assignment policies: a shared assignment policy (SAP) and a dedicated assignment policy (DAP). In the SAP, all aisles have a similar storage and demand profile, and they are all considered as regular aisles. In the DAP, the aisles are divided into fast-response (FR) aisles, close to the workstation, and regular aisles. Some robots are dedicated to the FR aisles, whereas the remaining robots are dedicated to the regular aisles. Within each group, the robots are shared among aisles, but a robot can only visit aisles to which it has been assigned. The inventory stored in the regular aisles is used to fulfill the low-priority orders. FR aisles are used to fulfill orders that must be delivered within short time windows (e.g., within two hours after ordering). FR aisles can be implemented in different ways. Typically, SKUs are dispersed over multiple storage locations (Lamballais, Roy, and De Koster 2020). This can be done purposefully, so that urgent items also have inventory in the FR aisles. Alternatively, products can be divided based on turnover speed, with fast movers stored in the FR aisles. In order to make a fair comparison between the two robot assignment strategies, we compare them with the same storage strategies within the different aisles, namely random or class based, and identical demand rates for each aisle in the two policies. The purposeful split of inventory over multiple storage locations to reduce response times is common in e-commerce warehouses, where very short lead times are required. If the average robot-to-aisle ratio of the FR aisles exceeds that of the regular aisles, a DAP will reduce the response time for the products stored in the FR aisles (albeit at the expense of the response time for products stored in the regular aisles). We investigate the effect of this trade-off between SAP and DAP and optimize the robot assignment under the DAP.

3.3. Blocking Policies in a CRSR System

Because the robots climb and descend bidirectionally within a rack section in an aisle, robot deadlock might occur, namely when two robots attempt to simultaneously access the same section in the rack or the opposite rack section in the same aisle. This may be prevented by waiting in front of the rack section when it is occupied by another robot. When driving in an aisle, at ground level, robots cannot overtake, and so, robot blocking can occur if a robot is waiting to enter a rack section that is occupied by another robot (see Figure 2).

We limit this blocking in the WOA policy by setting a threshold, O_b, to limit the maximum number of robots that can work in the same aisle at the same time. When the robot arrives at the entrance of the designated aisle, it examines the status of the aisle. If the number of robots working in the designated aisle is less than O_b, the arriving robot will enter the aisle. Otherwise, the arriving robot must wait outside the aisle. We assume there is sufficient waiting space outside the aisle. If a robot has completed its transactions and has departed from the aisle, one waiting robot can enter the aisle and move to the destination rack section (see the robots with dashed lines in Figure 3).

In the block-and-recirculate policy, we limit blocking as follows. When the robot arrives at the entrance of the aisle, it examines the status of the aisle. If the number of robots in the aisle (including the robots that are working in the designated aisle) is less than O_b, the arriving robot will move to the designated rack section and work in it. Otherwise, the robot circulates around the storage racks. When the robot has finished one loop, it examines the status of the aisle again. If the number of the robots in the aisle is still more than O_b, the robot keeps recirculating (see the robots with dotted lines in Figure 3).

4. Performance Evaluation Models for the CRSR System

In this section, we propose SOQNs to analyze a CRSR system with different policies. Then, we calculate the service time of the service nodes in the SOQNs.

4.1. SOQNs for the CRSR System with Different Policies

4.1.1. Shared Robot Assignment Policy with the Wait-Outside-Aisle Policy. We establish an SOQN with the shared robot assignment policy and the WOA policy considering both random and class-based storage policies and dual and single commands.

Figure 4 describes the system under the WOA policy with enough waiting buffers outside the aisles. The arriving order (a request for a tote) may wait for a robot to be transported, and a robot may also wait for an order. We use a synchronization node, *J*, to capture this synchronization between robots and orders. After the synchronization of the robot and an order, the robot moves from the workstation (its dwell point) to the entrance of designated aisle i with probability p_i^a, $(i = 1, 2, \cdots n_a)$. We assume that the value of p_i^a equals $1/n_a$ under SAP $(i = 1, 2, \cdots n_a)$. We use an infinite server (IS), μ_i^a, to model the robot travel from the dwell point to the entrance of the designated aisle i. Under the WOA policy, the robot will check the number of robots in the aisle when it arrives at the entrance of the aisle i. If the number of robots in the aisle is less than O_b, in the single-command cycle (retrieval), the arriving robot moves from the entrance of the aisle to the designated rack section (μ_l), retrieves a load in the designated rack (μ_s), and then moves from the bottom of the designated rack section to the exit of the aisle (μ_e); in the dual-command cycle (first storage and then retrieval), the arriving robot moves from the entrance of the aisle to the designated rack section (μ_l), stores the tote in the designated rack section (μ_d), moves to the designated retrieval rack section (μ_m), retrieves the tote in the rack (μ_s), and then moves from the bottom of the designated rack section to the exit of the aisle (μ_e). We use μ_b to present the operational steps in the aisle node. The station μ_b consists of O_b servers as the WOA policy allows a maximum O_b robots to work in the aisle at the same time. If the number of robots in the aisle reaches O_b, the arriving robot must wait outside the aisle (at the queuing of the node μ_b). From the exit of the aisle i, the robot moves to the workstation (service node μ_i^c, modeled as an infinite server) and is then processed at the workstation (service node μ_w) after possible queuing. In some cases, no waiting buffers exist outside the aisle. The detail information for the system without waiting buffers under the WOA policy can be found in Online Appendix B.

4.1.2. Dedicated Robot Assignment Policy with the Wait-Outside-Aisle Policy. We establish an SOQN with the dedicated robots assignment policy and the WOA policy considering both random and class-based storage policies and dual and single commands for the whole system (see Figure 5).

In the dedicated robot assignment policy, the aisles are divided into n_s FR aisles and n_r regular aisles ($n_s + n_r = n_a$). We use b_1 robots, which are assigned to serve FR aisles, and b_2 robots are assigned to serve regular aisle ($b_1 + b_2 = N$). The FR aisles are closer to the workstation, so even when $n_s/b_1 = n_r/b_2$, the performance of the FR aisles will be better than that of the regular aisles. After the synchronization of a robot and an order, the robot dedicated to the regular aisles moves to the entrance of the designated regular aisle r_i with probability $p_{r_i}^a$ $(i = 1, 2, \cdots n_r, p_{r_1}^a + p_{r_2}^a + \ldots + p_{r_{n_r}}^a = 1)$. The robot dedicated to the FR aisles moves to the entrance of the designated regular aisle s_i with probability $p_{s_i}^a$ $(i = 1, 2, \cdots n_s, p_{s_1}^a + p_{s_2}^a + \ldots + p_{s_{n_s}}^a = 1)$. The

Figure 3. Robot Blocking Policies (with $O_b = 3$)

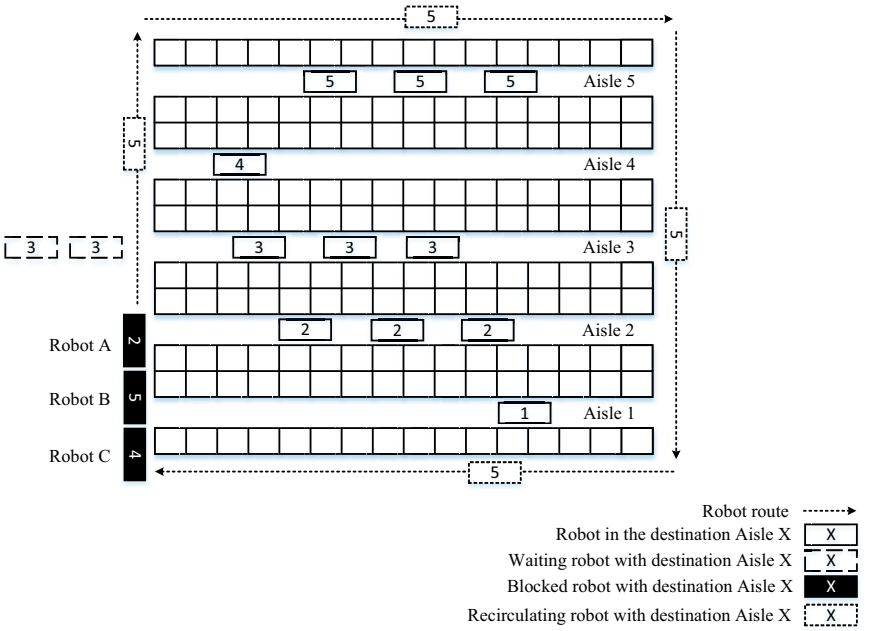

processes in the FR aisles and regular aisles are similar to those of the shared robot assignment policy.

4.1.3. Shared Robot Assignment Policy with the Block-and-Recirculate Policy. Figure 6 presents an SOQN for a CRSR system with the BAR policy and the shared robot assignment policy. After the synchronization of a robot and an order, the robot moves from the workstation to the entrance of designated aisle i with probability p_i^a $(i = 1, 2, \cdots n_a)$. We use μ_i^a to model the movement from the workstation to the entrance of the designated aisle i. When the robot arrives at the entrance of the designated aisle, it examines the number of robots in it. If the number of robots in the designated aisle is less than O_b, the robot goes into the aisle and works in the designated rack section. We use μ_b to present the operation in the aisle. It is defined as in Section 4.1.1. Because the aisle can allow a maximum O_b robots working in it, the station μ_b has O_b servers. If the number of robots in the

Figure 4. Semiopen Queueing Network with the Shared Robot Assignment Policy and the Wait-Outside-Aisle Policy with Waiting Buffers

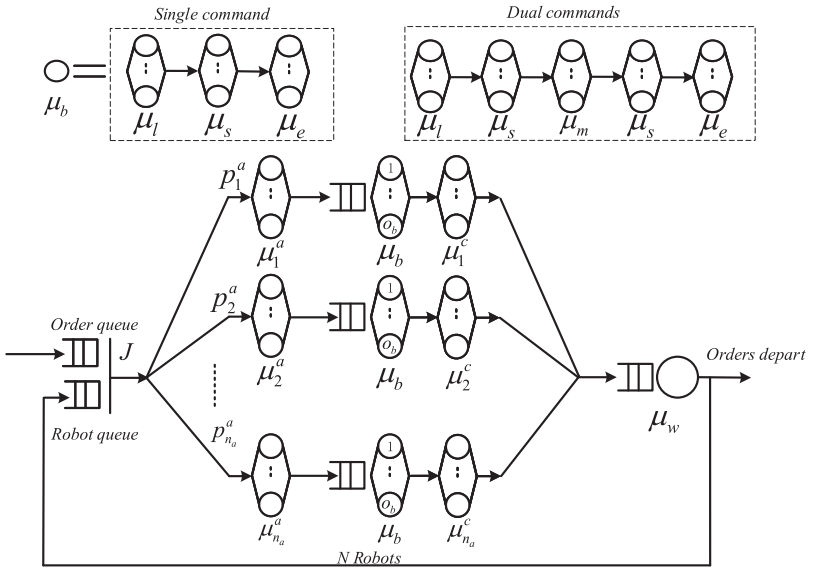

Figure 5. Semiopen Queueing Network with the Dedicated Robot Assignment Policy and the Wait-Outside-Aisle Policy

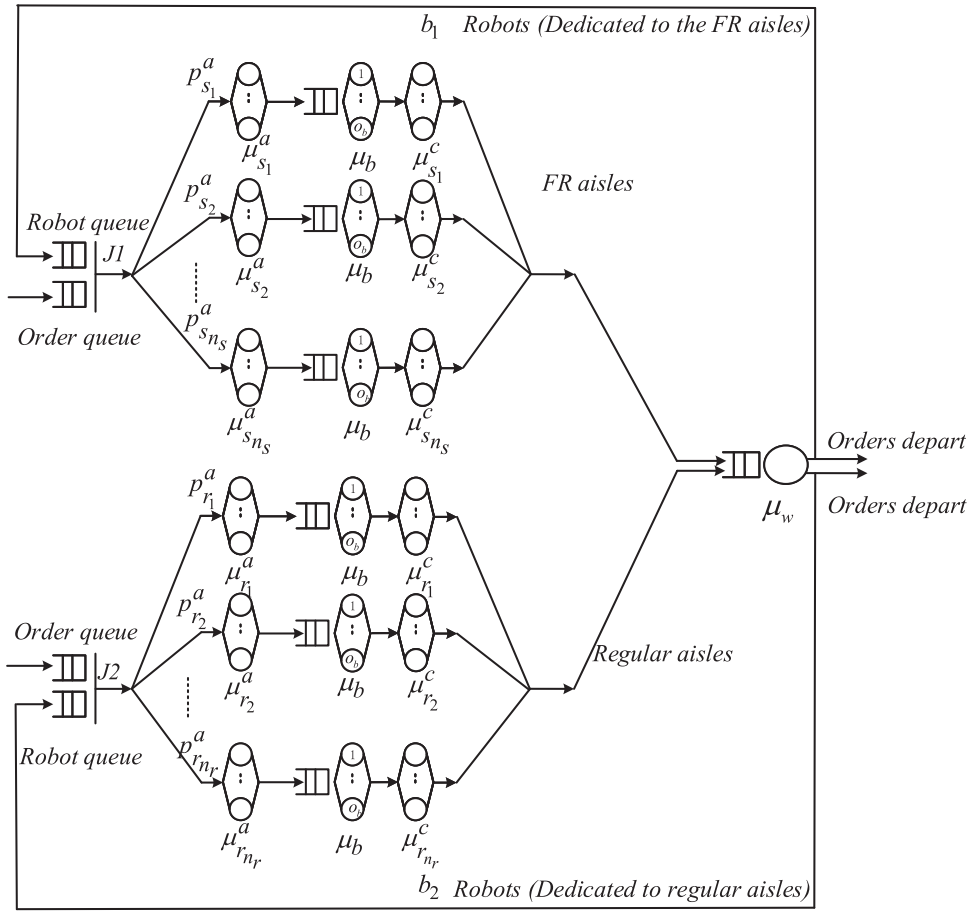

designated aisle reaches O_b, the robot recirculates in the system. We use μ_i^h to denote that the robot recirculates around the perimeter of the system from the entrance of the aisle i to the workstation (see the single-directional recirculating path in Figure 3). Nodes μ_i^h and μ_i^a form the total recirculation path. If the robot finishes the operation in the aisle, the robot moves from the exit of the aisle i to the workstation (service node μ_i^c) and is then processed of the workstation (service node μ_w).

4.1.4. Dedicated Robot Assignment Policy with the Block-and-Recirculate Policy. We establish an SOQN with the dedicated robot assignment policy and the block-and-recirculate policy considering both random and class-based storage policies and dual and single commands for the whole system (see Figure 7). After the synchronization of a robot and an order, the robot dedicated to the FR aisles moves to the entrance of the FR aisles or regular aisles. We use b_1 to denote robots dedicated to the FR aisles, and b_2 robots are dedicated to the regular aisles ($b_1 + b_2 = N$). The following processes are similar to the model for the shared robot assignment policy.

4.2. Service Time Expressions

Based on Section 3.1, the main operational steps are as follows.

Step a. The robot moves from the workstation to the entrance of aisle i (service node μ_i^a).

Step b. The robot works in the designated aisle (service node μ_b) in single-command or dual-command model.

Step c. The robot moves from the exit of the aisle i to the workstation (service node μ_i^c).

Step d. The worker loads/unloads the tote at the workstation (service node μ_w).

The origin point (0, 0, 0) is the left bottom corner of the system. The coordinates of the workstation are (x_w, y_w, z_w). Because the workstation is located in the bottom center of the system (see Figure 1), the coordinates of workstation are given by Equation (4):

$$x_w = \frac{n_l l}{2} + w_c, \qquad y_w = 0, \qquad z_w = 0. \tag{4}$$

Figure 6. Semiopen Queueing Network in the Shared Robot Assignment Policy with the Block-and-Recirculate Policy

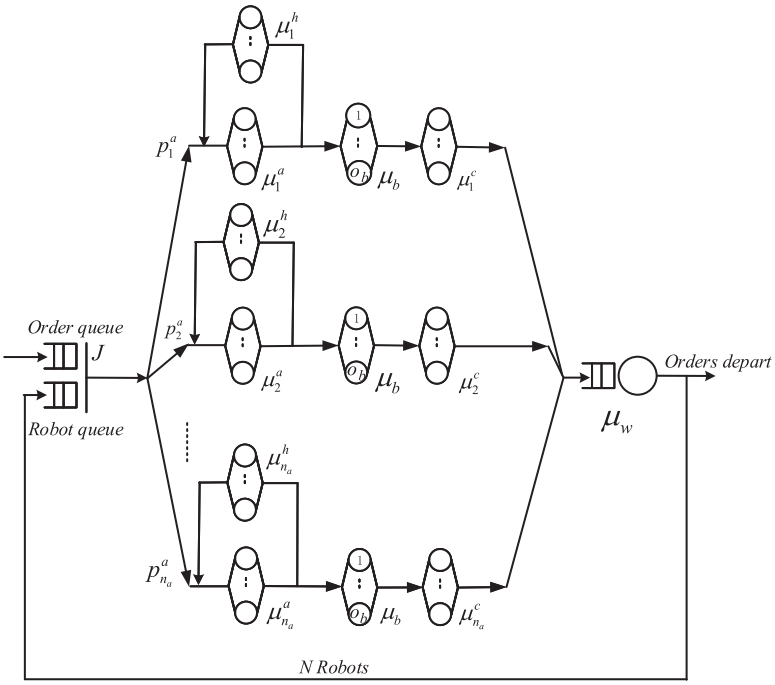

4.2.1. Service Time Expressions Under the Wait-Outside-Aisle Policy.

Step a. Denote the coordinates of the entrance of the aisle i as $(x_{a_i}, y_{a_i}, z_{a_i})$, which are given by Equation (5):

$$\begin{aligned} &x_{a_i} = w_c, \\ &y_{a_i} = w_c - w - \frac{w_a}{2} + (w_a + 2w)i, \quad i = 1,2, \cdots n_a, \\ &z_{a_i} = 0. \end{aligned} \tag{5}$$

Let D_{a_i} be the travel distance between the workstation and the entrance of the aisle i. We have

$$\begin{aligned} D_{a_i} &= |x_{a_i} + x_w| + |y_{a_i} - y_w| + |z_{a_i} - z_w| \\ &= \frac{n_l l}{2} + \frac{6w_c - w_a - 2w}{2} + (w_a + 2w)i, \quad i = 1,2, \cdots n_a. \end{aligned} \tag{6}$$

Let T_{a_i} be the travel time from the workstation to the entrance of the aisle i. We have

$$\begin{aligned} T_{a_i} &= \frac{D_{a_i}}{v_h} \\ &= \frac{n_l l}{2v_h} + \frac{6w_c - w_a - 2w}{2v_h} + \frac{(w_a + 2w)i}{v_h}, \quad i = 1,2, \cdots n_a. \end{aligned} \tag{7}$$

The expectation and squared coefficient of variation (SCV) of service time T_{a_i} are

$$\mu_i^{a^{-1}} = E[T_{a_i}] = \frac{n_l l}{2v_h} + \frac{6w_c - w_a - 2w}{2v_h} + \frac{(w_a + 2w)i}{v_h}, \quad i = 1,2, \cdots n_a \tag{8}$$

$$cv_i^{a^2} = \frac{E[T_{a_i}^2] - E[T_{a_i}]^2}{E[T_{a_i}]^2} = 0. \tag{9}$$

Step b. We denote the coordinates of the retrieval position as (x_s, y_s, z_s), which are given by Equation (10):

$$\begin{aligned} &x_s = w_c + lj, \quad j = 1,2, \cdots n_l, \\ &y_s = w_c - w - \frac{w_a}{2} + (w_a + 2w)i, \quad i = 1,2, \cdots n_a, \\ &z_s = kh, \quad k = 1,2, \cdots n_h. \end{aligned} \tag{10}$$

Denote the coordinates of the bottom of the designated rack section as (x_b, y_b, z_b), which are given by Equation (11):

$$\begin{aligned} &x_b = w_c + lj, \quad j = 1,2, \cdots n_l, \\ &y_b = w_c - w - \frac{w_a}{2} + (w_a + 2w)i, \quad i = 1,2, \cdots n_a, \\ &z_b = 0. \end{aligned} \tag{11}$$

We use T_s to denote the service time of the robot in the designated rack section, including climbing to the designated position, retrieving the tote, and descending to the aisle. We can obtain T_s by Equation (12):

$$\begin{aligned} T_s &= 2 \times \frac{|x_s - x_b| + |y_s - y_s| + |z_s - z_b|}{v_v} + t \\ &= \frac{2hk}{v_v} + t, \quad k = 1,2, \cdots n_h. \end{aligned} \tag{12}$$

Note that node μ_l and μ_e are ISs and that the sum of μ_l and μ_e is constant, $n_l l / v_h$. We use T_b to denote the

Figure 7. Semiopen Queueing Network in the Dedicated Robot Assignment Policy with the Block-and-Recirculate Policy

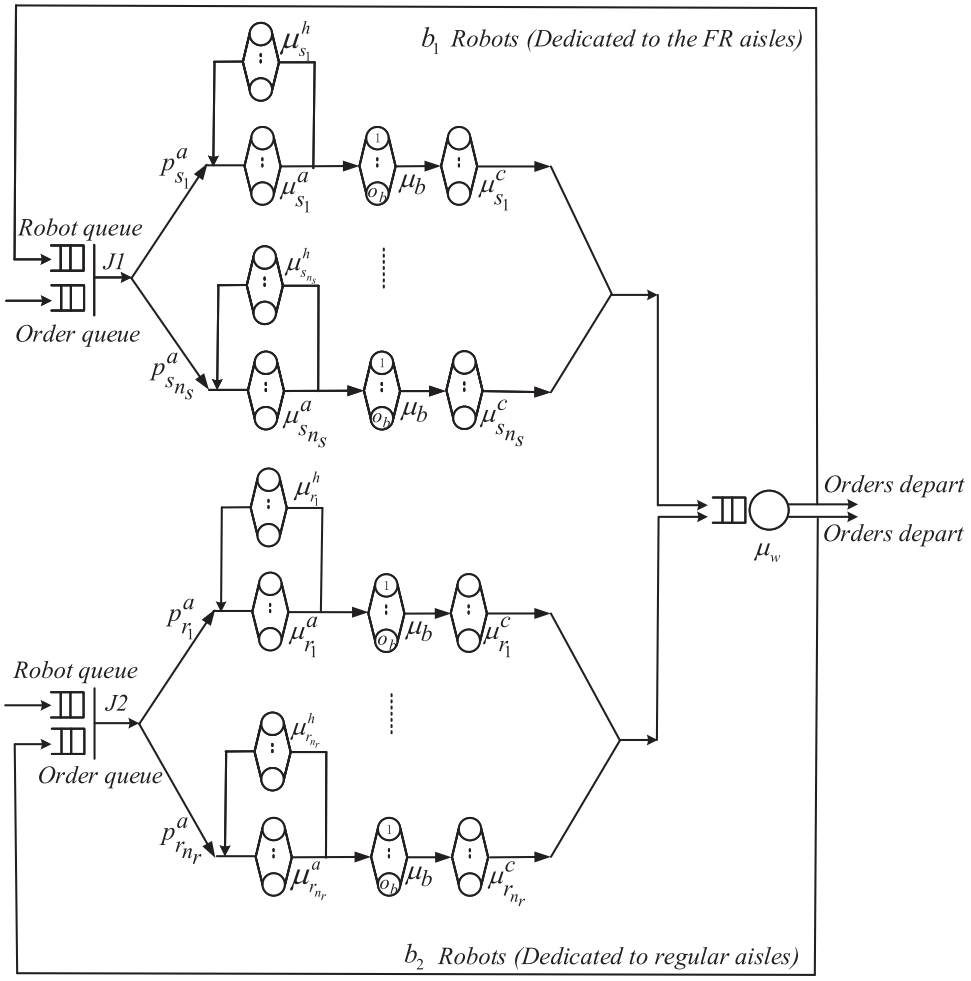

service time in the designated aisle. For the random storage policies, the first and second moments of T_b can be calculated as the following equations:

$$E[T_b] = \sum_{k=1}^{n_h}\left(\frac{2hk}{v_v}+t+\frac{n_l l}{v_h}\right)\times\frac{1}{n_h} = \frac{hn_h+h}{v_v}+\frac{n_l l}{v_h}+t \tag{13}$$

$$E[T_b^2] = \sum_{k=1}^{n_h}\left(\frac{2hk}{v_v}+t+\frac{n_l l}{v_h}\right)^2\times\frac{1}{n_h} = \frac{2(n_h+1)(2n_h+1)h^2}{3v_v^2}+\left(t+\frac{n_l l}{v_h}\right)^2+\frac{2h(tv_h+n_l l)(n_h+1)}{v_v v_h}. \tag{14}$$

The SCV of T_b can be calculated by

$$cv_b^2 = \frac{E[T_b^2]-E[T_b]^2}{E[T_b]^2} = \frac{v_h^2h^2(n_h^2-1)}{3(ln_l v_v+v_h(h+hn_h+tv_v))^2}. \tag{15}$$

Under the class-based storage policy, the probability that the tote belongs to a specific class can be calculated by the following equations:

$$P_A = \frac{N_{sp}^A F_A}{N_{sp}^A F_A+N_{sp}^B F_B+N_{sp}^C F_C},$$
$$P_B = \frac{N_{sp}^B F_B}{N_{sp}^A F_A+N_{sp}^B F_B+N_{sp}^C F_C},$$
$$P_C = \frac{N_{sp}^C F_C}{N_{sp}^A F_A+N_{sp}^B F_B+N_{sp}^C F_C}. \tag{16}$$

We use P_k to denote the probability that the retrieval position belongs to tier k. We can get P_k as follows:

$$P_k = \begin{cases} \frac{P_A}{n_A}, & \text{if } 1\le k\le n_A, \\ \frac{P_B}{n_B}, & \text{if } n_A+1\le k\le n_A+n_B, \\ \frac{P_C}{n_C}, & \text{if } n_A+n_B+1\le k\le n_h. \end{cases} \tag{17}$$

The first and second moments of the service time μ_b under the class-based storage policy are given:

$$E[T_b] = \sum_{k=1}^{n_h}\left(\frac{2hk}{v_v} + t + \frac{n_l l}{v_h}\right) \times P_k \tag{18}$$

$$E[T_b^2] = \sum_{k=1}^{n_h}\left(\frac{2hk}{v_v} + t + \frac{n_l l}{v_h}\right)^2 \times P_k. \tag{19}$$

Then, the SCV of process μ_b under the class-based policy can be calculated by

$$cv_b^2 = \frac{E[T_b^2] - E[T_b]^2}{E[T_b]^2}. \tag{20}$$

In dual-command node, the robot first moves to the rack section of the designated storage position and after finishing the storage, then moves to the rack section of the designated retrieval position. We denote the coordinates of the designated retrieval position as (x_d, y_d, z_d). The travel time, T_m, from the bottom of the designated storage rack section to the bottom of the designated retrieval rack section is as follows:

$$T_m = \frac{|x_d - x_b|}{v_h}, \quad \text{where } x_d, x_b = lj,\ j = 1, \ldots, n_l. \tag{21}$$

The expectation and SCV of μ_m are shown in Equations (22) and (23):

$$\mu_m^{-1} = E[T_m] = \frac{2l}{v_h}\sum_{i=1}^{n_l}\sum_{j=1}^{i}(i-j)\frac{1}{n_l^2} = \frac{(n_l+1)(n_l-1)l}{3n_l v_h} \tag{22}$$

$$cv_m^2 = \frac{E[T_m^2] - E[T_m]^2}{E[T_m]^2}. \tag{23}$$

Then, we can use equations similar to Equations (18) and (19) to get the expectation and SCV of μ_b under the dual-command mode and random storage policy:

$$\mu_b^{-1} = E[T_b] = \sum_{k_1=1}^{n_h}\sum_{k_2=1}^{n_h}\sum_{i=1}^{n_l}\sum_{j=1}^{i}\left(\frac{n_l l}{v_h} + 2t + \frac{2hk_1}{v_v} + \frac{2hk_2}{v_v} + (i-j)\frac{2l}{v_h}\right) \times \frac{1}{n_h^2 n_l^2} \tag{24}$$

$$cv_b^2 = \frac{E[T_b^2] - E[T_b]^2}{E[T_b]^2}, \tag{25}$$

where

$$E[T_b^2] = \sum_{k_1=1}^{n_h}\sum_{k_2=1}^{n_h}\sum_{i=1}^{n_l}\sum_{j=1}^{i}\left(\frac{n_l l}{v_h} + 2t + \frac{2hk_1}{v_v} + \frac{2hk_2}{v_v} + (i-j)\frac{2l}{v_h}\right)^2 \times \frac{1}{n_h^2 n_l^2}. \tag{26}$$

The expectation and SCV of μ_b under the dual-command mode and class-based storage policy can be calculated and are given in Equations (27) and (28):

$$E[T_b] = \sum_{k_1=1}^{n_h}\sum_{k_2=1}^{n_h}\sum_{j=1}^{i}\sum_{i=1}^{n_l}\left(\frac{n_l l}{v_h} + 2t + \frac{2hk_1}{v_v} + \frac{2hk_2}{v_v} + (i-j)\frac{2l}{v_h}\right) \times \frac{P_k^2 1}{n_l^2} \tag{27}$$

$$cv_b^2 = \frac{E[T_b^2] - E[T_b]^2}{E[T_b]^2}, \tag{28}$$

where

$$E[T_b^2] = \sum_{k_1=1}^{n_h}\sum_{k_2=1}^{n_h}\sum_{j=1}^{i}\sum_{i=1}^{n_l}\left(\frac{n_l l}{v_h} + 2t + \frac{2hk_1}{v_v} + \frac{2hk_2}{v_v} + (i-j)\frac{2l}{v_h}\right)^2 \times \frac{P_k^2 1}{n_l^2}. \tag{29}$$

Step c. The travel time from the exit of the aisle i to the workstation can be calculated as follows:

$$T_{c_i} = \frac{|x_{e_i} + x_w| + |y_{e_i} - y_w| + |z_{e_i} - z_w|}{v_h} = \frac{n_l l}{2v_h} + \frac{6w_c - w_a - 2w}{2v_h} + \frac{(w_a + 2w)i}{v_h}, \quad i = 1, 2, \cdots n_a. \tag{30}$$

The expectation and SCV of service time of T_{c_i} are

$$\mu_i^{c^{-1}} = E[T_{e_i}] = \frac{6w_c - w_a - 2w}{2v_h} + \frac{(w_a + 2w)i}{v_h} + \frac{n_l l}{2v_h}, \quad i = 1, 2, \cdots n_a \tag{31}$$

$$cv_i^{c^2} = \frac{E[T_{c_i}^2] - E[T_{c_i}]^2}{E[T_{c_i}]^2} = 0. \tag{32}$$

Step d. The service time at the workstation is a short duration. Therefore, the expectation and SCV of the service time at the workstation are as follows:

$$\mu_w^{-1} = t_w, \qquad cv_w^2 = 0. \tag{33}$$

4.2.2. Service Time Expressions Under the Block-and-Recirculate Policy. The expected value and SCV of the service time at the workstation (μ_w, cv_w^2), the robot moving time from the workstation to the entrance of the designated aisle (μ_i^a, $cv_{a_i}^2$), the robot moving time from the exit of the aisle to the workstation (μ_i^c, $cv_{c_i}^2$), and the main time in the aisle (μ_b, cv_b^2) have the same value as under the WOA policy.

Based on the recirculating policy, the expectation and SCV of μ_i^h can be calculated by

$$\mu_i^{h^{-1}} = \frac{3w_c + n_l l}{v_h} + \frac{4wn_a + 2w_a n_a + w_a + 2w}{v_h} - \frac{(w_a + 2w)i}{v_h}, \quad i = 1, 2, \cdots n_a \tag{34}$$

$$cv_i^{h^2} = 0. \tag{35}$$

5. Solution Approach

Section 5 provides the solution approaches to solve the SOQNs proposed in Section 4. Section 5.1 shows the solution approach to solve the SOQN with the BAR policy. The solution approach for the system under the WOA policy can be found in Online Appendix C, and the solution approach for the system under the BAR policy can be found in Online Appendix D. Section 5.1 presents an algorithm to solve the SOQN with the BAR policy. Section 5.2 presents simulation validation.

5.1. Solution Approach of the SOQN with the Block-and-Recirculate Policy

The semiopen queueing network under the BAR protocol in Figure 6 does not have a product form solution. Therefore, we approximate the network by another one with the jump-over blocking protocol (Van Dijk 1988). As shown by Van der Gaast et al. (2020), the jump-over blocking protocol admits a product-form stationary queue length distribution for a network with jump-over nodes and allows an accurate estimation of the performance measures.

We use μ_i^b to denote the operation in aisle i all with the same service time ($\mu_1^b = \mu_2^b = \ldots \mu_{n_a}^b = \mu_b$). A robot can be tagged as "visited μ_i^b" if the robot visits node aisle i or "left μ_i^b" if the robot does not visit aisle i. For example, a robot is tagged "left μ_i^b" if the number of the robots in the designated aisle i reaches O_b and the robot should recirculate instead of entering the designated aisle. Otherwise, the robot can be tagged as "visited μ_i^b." However, the robot can be tagged as "visited μ_i^b" with zero incurred service time if the number of the robots in the aisle i reaches O_b. Therefore, the robots can be tagged randomly without the consideration that the robot actually visits or leaves μ_i^b. We use p_i^b to denote the blocking probability of aisle i in the original network. In the jump-over network, the probability of a robot tagged as "left μ_i^b" equals the block probability, p_i^b, and so, the probability of a robot tagged as "visited μ_i^b" equals $1 - p_i^b$. Although the value of p_i^b is unknown at the beginning, it can be estimated by an initial value between zero and one, followed by successive updates in an iteration algorithm until the convergence (see Section 5.2). For example, we initialize p_i^b as zero. With the current parameters (see Table 3) for the system with a single command and a random storage policy, 22 iterations are needed for obtaining a value of p_i^b, accurate in seven decimal places. Hence, we can assume that p_i^b is known beforehand in the jump-over network. Therefore, with probability $1 - p_i^b$, the robot from μ_i^a is tagged as "visited μ_i^b" and then, visits node μ_i^c. With probability p_i^b, the robot from μ_i^a is tagged as "left μ_i^b" and then, visits node μ_i^h. The corresponding jump-over approximation of the SOQN is presented in Figure 8.

5.2. Simulation Validation

We build simulation models to validate the accuracy and effectiveness of our analytical models. Instead of simulating the queueing networks, we simulate a realistic implementation of an actual system. We use Flexsim software v19.0.0 (Flexsim 2019) to establish the simulation models. The simulation models can capture the physical three-dimensional movement of the robots for the different policies. The system parameters are presented in Table 3 and are obtained by estimations based on the Exotec Solutions video (Exotec Solutions 2019; Exotec 2020a, b). The arrival rate equals $400/h$. We assume the value of $O_b = 3$. For the class-based storage policy, we have $(P_A, P_B, P_C) = (0.65, 0.25, 0.1)$. The system throughput time (T_o), the order waiting time (W_r), and the robot utilization (ρ) obtained by simulation and the analytical model are compared. For each scenario, 20 replications are run with a warm-up period of 10 hours and a run time of 100 hours per replication. A detailed description of the simulation model is provided in Online Appendix E. We calculate the accuracy of the analytical models by $\delta\% = |A - S|/S \times 100\%$, where $\delta\%$ is the relative error. A and S are the analytical and simulation results, respectively. The error range for δ can be found in Online Appendix E. Because in the most cases, the waiting buffers always exit outside the system, except with the special instruction, WOA means the waiting policy with enough waiting buffers.

6. Numerical Analysis

Choosing the right operating policies impacts the system performance. In Section 6.1, we investigate the effect of the blocking policies. In Section 6.2, we study the performance of the different robot assignment policies. In addition, the layout configuration may impact the system performance. Therefore, we investigate the effect of different rack dimensions in Section 6.3.

6.1. Analyzing the Effect of the Blocking Policies

In this section, we compare the impact of the WOA and BAR policies on the order throughput under single command and a random storage policy (see Figure 9). The system parameters with five aisles are the same as in Table 3. We vary the number of robots in the system from three to nine and the maximum number of robots that can simultaneously work in an aisle (O_b) from one

Table 3. System Parameters

w	w_c	w_a	l	h	n_a	n_s	n_r	n_h	n_l	t	t_w	v_h	v_v	N	b_1	b_2
0.8 m	2.45 m	0.96 m	0.66 m	0.33 m	5	2	3	11	16	1.4 seconds	3.6 seconds	1.5 m/s	1 m/s	7	3	4

to five, respectively, and we observe the order throughput obtained by different scenarios. We also set $O_b = \infty$ to evaluate the system without blocking.

Based on Figure 9, the WOA policy with sufficient waiting space in the aisle buffers outperforms the BAR policy because the recirculation in the BAR policy takes a lot of time. With an increase in O_b, the system throughput under the WOA policy is close to that of the system without any blocking. For $O_b = 5$, they almost coincide (see Figure 9(c)).

The WOA policy without robot waiting buffers only outperforms BAR when the number of robots is small. With an increase in the number of robots, the system throughput of WOA without waiting buffers decreases sharply. This is because of blocked robots, which may block other robots outside the aisles. When O_b is small, this throughput decrease is more obvious. When the number of robots is large, BAR outperforms WOA without waiting buffers because blocked robots can still recirculate without blocking other robots.

We conclude that for the system with unlimited waiting buffer space, the WOA performs better than the BAR policy. For a system with limited waiting space, the choice of WOA and BAR depends on the number of robots in the system and the throughput requirement. BAR may be a better choice for systems with limited waiting space for robots.

6.2. Analyzing the Effect of the Different Robot Assignment Policies

In this section, we first compare the throughput time under the SAP and the DAP. Then, we optimize the assignment of robots under DAP considering a fairness constraint between the FR aisles and the regular aisles and the priority of the FR aisles.

6.2.1. Comparison of the Different Robot Assignment Policies. We vary the number of robots dedicated to FR and regular aisles (b_1 robots dedicated to FR aisles and b_2 robots dedicated to regular aisles) to investigate the system throughput time (in seconds). We set the number of FR and regular aisles as four ($n_s = n_r = 4$), with equal order arrival rates ($240/h$). Under dual commands, the minimum number of robots needed to make the system stable equals 12, which is larger than the minimum number of robots under single commands, 10. Other system parameters are the same as shown in Table 3. Because the WOA policy performs best in most cases, we only consider the WOA policy in the comparison. Figure 10 shows the throughput time for the FR and regular aisles for single- and dual-command policies, different robot-to-aisle distributions, and different levels of O_b. Also, the throughput time is shown for the case of only regular aisles under SAP (see the horizontal dotted line with star in Figure 10). Based on Figure 10, (a)–(c), we find that under single commands, the throughput time

Figure 8. Jump-Over Approximation of the Semiopen Queueing Network in the Shared Robot Assignment Policy with the Block-and-Recirculate Policy

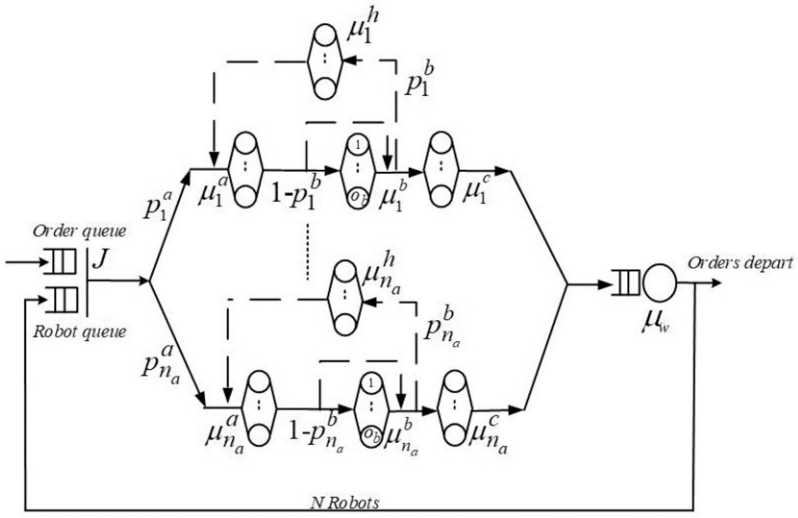

Figure 9. Comparison Results of the WOA and BAR Policy

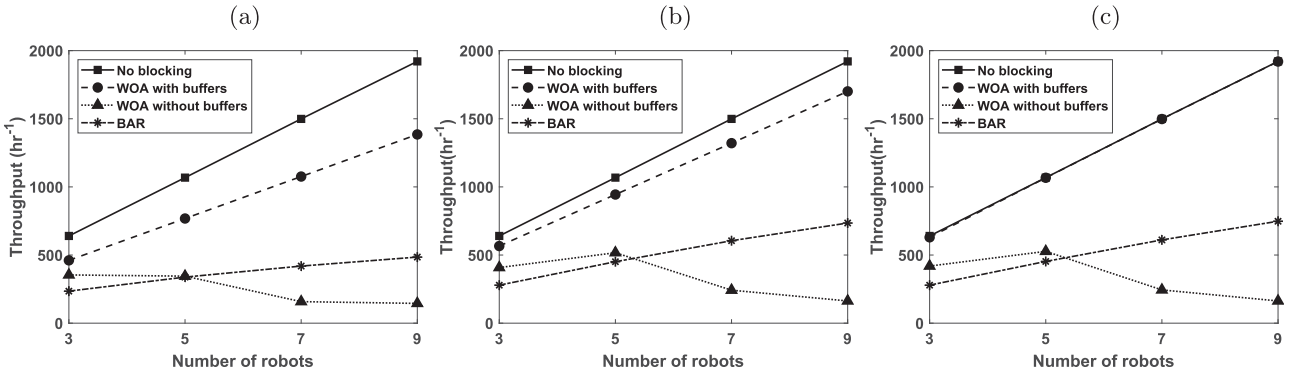

Notes. (a) $O_b = 1$. (b) $O_b = 3$. (c) $O_b = 5$.

for FR aisles is always less than regular aisles even when the robot-to-aisle ratio of regular aisles is larger than that ratio of the FR aisles (i.e., four robots dedicated to FR aisles and six robots dedicated to regular aisles). This is because the FR aisles are closer to the workstation and the mean horizontal travel time of the robots dedicated to the FR aisles is less than that of the regular aisles. For the same reason, under the dual-command mode, when the robot-to-aisle ratios of FR and regular aisles are identical, the FR aisles have a shorter mean throughput time than that of regular aisles (i.e., six robots dedicated to FR aisles and six robots dedicated to regular aisles). When the robot-to-aisle ratio for the regular aisles doubles that of the FR aisles (i.e., four robots dedicated to FR aisles and eight robots dedicated to regular aisles), the regular aisles have a shorter throughput time than the FR aisle. Figure 10 also shows that the system is more sensitive to the robot-to-aisle ratio than to the value of O_b. It is because the robot-to-aisle ratio impacts not only the mean service time in the aisle but also, the mean horizontal travel time from the workstation to the aisle. Also, for the farthest aisle, the horizontal travel time takes a larger fraction of the total travel time for other aisles.

To sum up, when the ratio of the number of robots to the number of FR aisles is the same as that of the regular aisles, the mean order throughput time in the FR aisles is shorter because FR aisles are closer to the workstation. Therefore, the robots dedicated to the FR aisles have a shorter expected travel time. For the system parameters investigated, the regular aisles have a shorter mean order throughput time than the FR aisles when the ratio of robots to aisles doubles that of the FR aisles. These results show that the DAP can be attractive for a warehouse where fast delivery for certain products is required (i.e., with few "fast-response" aisles). The SAP can be an attractive policy for a warehouse when no particular delivery priority is required because this policy is fair for all orders.

We also combine robot assignment policies and storage policies in a full factorial manner to investigate how these policies impact the throughput time. We set the value of the maximum allowed number of robots entering an aisle as 1 and investigate the system with 10 aisles and 14 robots under single command. In Figure 11, the x axis shows the results for two storage policies, class based and random, with 10% FR orders and 10% FR aisles (Figure 11(a)) and with 20% FR orders and 20% FR aisles (Figure 11(b)). Note that we assume x% of the orders to be FR, with x% of the aisles to be allocated to FR storage. However, with x% FR orders and x% of the aisles allocated to FR storage, the graphs of the FR policy with random robot assignment and those of SAP are identical. The legend in Figure 11 is the same as in Figure 10. The class-based storage policy is always better than the random storage policy. However, the lines for the different robot assignment policies are not parallel. This suggests an interaction between the storage policy and the robot assignment policy. Figure 11 shows that the mean throughput time of fast-response aisles under the DAP is always shorter than that under the SAP, whereas the throughout time of regular aisles under the DAP hardly suffers, assuming a class-based storage strategy. The DAP can, therefore, realize a fast delivery of the priority orders.

6.2.2. Optimization of Robot Assignment Under Dedicated Policy. Our model can help to determine the number of robots b_1^* that should be assigned to the FR aisles to satisfy a maximum allowed throughput time with the smallest impact on regular aisles. Under the single- and dual-command modes, the maximum allowed throughput times for FR aisles are $\overline{T_s}$ and $\overline{T_d}$, respectively. We use $T_s(b_1)$ and $T_s(b_2)$ to denote the throughput time for FR with b_1 robots and regular aisles with b_2 robots under the single-command mode,

Figure 10. Comparison Results of the SAP and DAP Policies

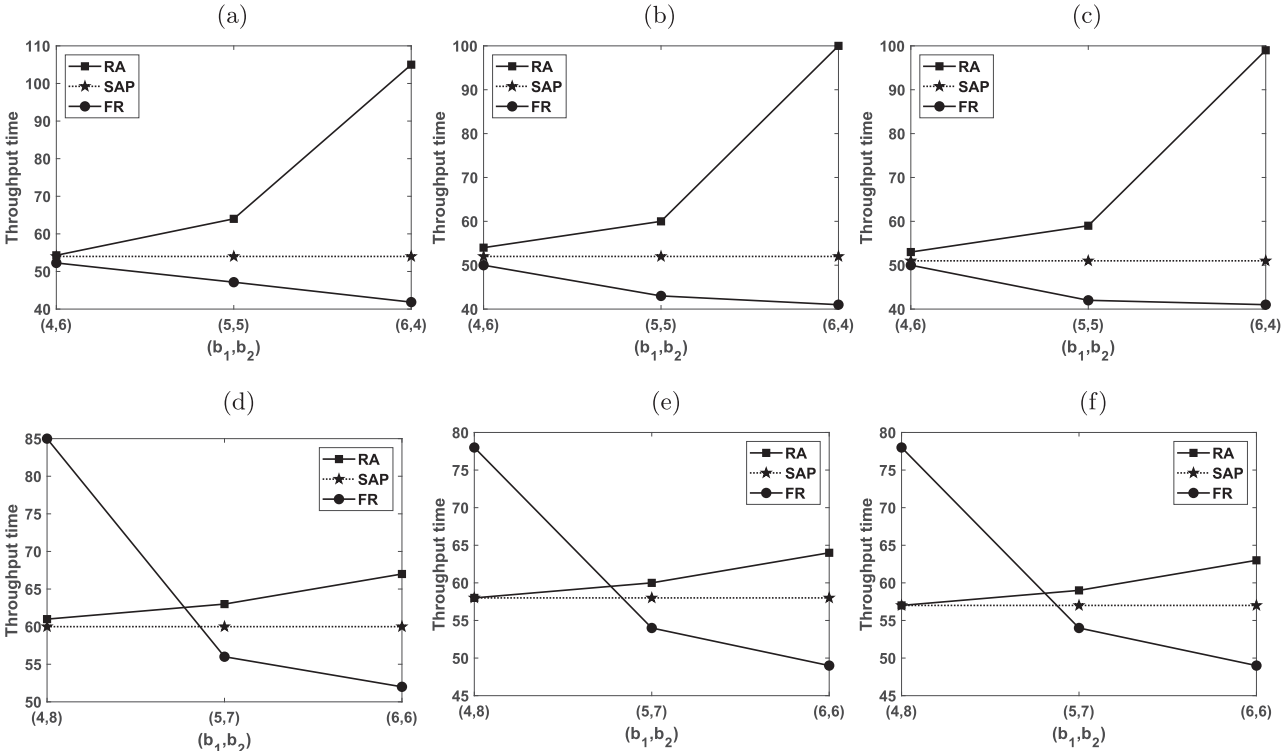

Notes. (a) Single, $O_b = 2$. (b) Single, $O_b = 3$. (c) Single, $O_b = 4$. (d) Dual, $O_b = 2$. (e) Dual, $O_b = 3$. (f) Dual, $O_b = 4$. Single indicates single command. Dual indicates dual command. RA, regular aisles.

respectively. We use $T_d(b_1)$ and $T_d(b_2)$ to denote the throughput time for FR with b_1 robots and regular aisles with b_2 robots under the dual-command mode, respectively. The objective is to minimize $|T_s(b_1) - T_s(b_2)|$ for the fairness between FR and regular aisles and $T_s(b_1) \le \overline{T_s(b_1)}$ for the fast response of the FR aisles. Thereby, the decision system to calculate decision variables on b_1 can be formulated as, under single command,

$$\min : |T_s(b_1) - T_s(b_2)|$$
$$\text{subject to (s.t.) } T_s(b_1) \le \overline{T}_s.$$

Under dual command,

$$\min : |T_d(b_1) - T_d(b_2)|$$
$$\text{s.t. } T_d(b_1) \le \overline{T}_d.$$

For example, under single commands, let the maximum allowed throughput time for an FR aisle be $\overline{T}_s =$

Figure 11. The Impact of the Different Policies on the System Throughput Time

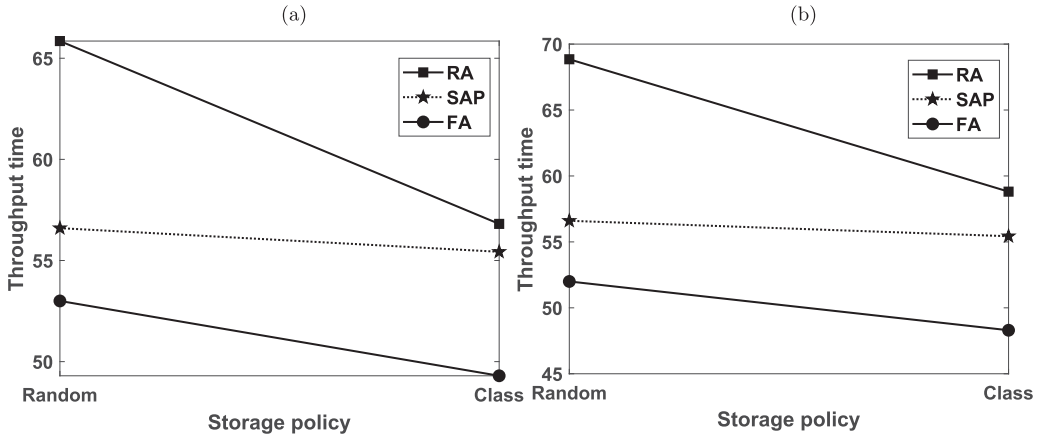

Notes. (a) 10% priority orders. (b) 20% priority orders. RA, regular aisles.

45 seconds in the examined warehouse (with eight aisles and other parameters as in Table 3). Based on Figure 10, the warehouse manager can assign five or six robots to meet the time bound of the FR aisles. Considering both the fairness between FR and regular aisles and the priority measured by the maximum allowed throughput time of FR aisles, the optimal number of robots assigned to FR aisles, b_1^*, is four.

6.3. Optimal Rack Dimensions

We study the optimal rack shape ratio (expected maximum horizontal travel time, $n_l l/v_h$, compared with the expected maximum vertical travel time, $n_h \times h/v_v$) for a CRSR system with one aisle in the single-command mode and random storage policy with the objective to maximize the system throughput capacity under different blocking policies (THC_{BAR}, THC_{WOA}). The number of storage positions (C_0) and the number of robots (N) are given. Other system parameters are the same as shown in Table 3. We estimate the system throughput capacity through the closed queuing networks built by removing the synchronization node of the SOQNs. In each scenario, the system throughput capacity is calculated while changing the number of tiers (n_h) and rack (n_l) sections from their lower bounds (L_h and L_l denote the lower bounds for the number of tiers and rack sections, respectively) to their upper bounds (U_h and U_l, respectively) such that the total number of storage positions ($C_0 = 108$) remains the same. The decision model to calculate the optimal rack dimension can be formulated as

$$\begin{aligned} &\max\ THC_{BAR} \\ &\max\ THC_{WOA} \\ &\text{s.t.} \begin{cases} L_h \le n_h \le U_h \\ L_l \le n_l \le U_l \\ C_0 = n_h n_l \\ C_0, L_h, U_h, L_l, U_l \text{ are given.} \end{cases} \end{aligned}$$

Under both blocking policies, we study two levels of the number of robots in the system with $n = 4$, 8 and four levels of the maximum allowed number of robots working in the aisle at the same time with $O_b = 1, 2, 3, 4$. Because n_l and n_h only take integer values, only certain optimal rack shape ratios can be investigated. Figure 12 illustrates the system throughput for different scenarios. Based on Figure 12, we find that under both WOA and BAR policies, the system can reach the maximum throughput when the optimal rack shape ratio satisfies $n_h h/v_v = n_l l/v_h$ (= 3.96 with current parameters), corresponding to an optimal height-to-length ratio of 0.67. This optimal rack shape ratio of height to length is insensitive to the number of robots and the value of the maximum

Figure 12. System Throughput in Different Scenarios

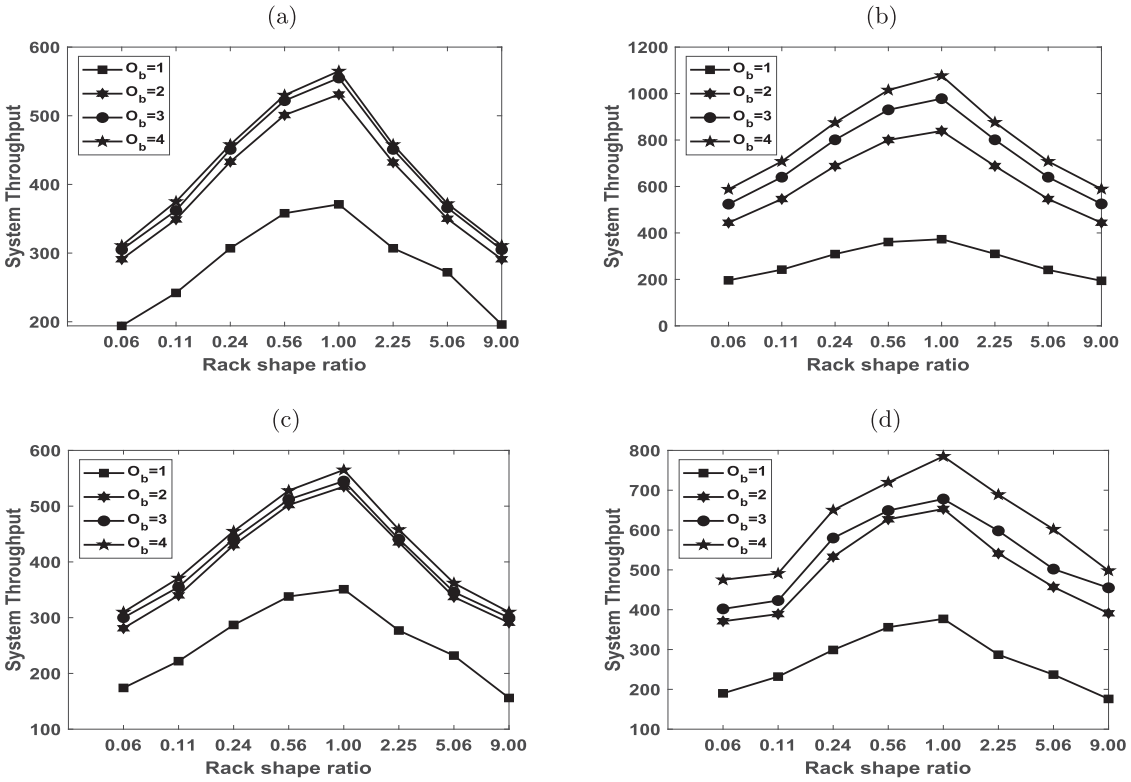

Notes. (a) $N = 4$, WOA. (b) $N = 8$, WOA. (c) $N = 4$, BAR. (d) $N = 8$, BAR.

allowed number of robots working in the aisle at the same time.

7. Conclusions and Future Work

We investigate a new robotic material-handling system: the CRSR system. The system has not been studied before and is modeled using SOQNs, with different operating policies. We contribute by formulating these models and design insights. The analytical models are validated using simulation. We investigate two robot blocking policies: the WOA policy and the BAR policy. With our scenario, if the system has waiting buffers outside the aisle, the WOA policy achieves a larger order throughput than the BAR policy. If the system does not have waiting buffers, the WOA has a larger order throughput than the BAR when the number of robots is small. With an increase in the number of robots, the WOA has a smaller order throughput than the BAR. We also compare the SAP and the DAP. Even the DAP has longer throughput time for regular aisles; it can shorten the throughput time for fast-response aisles. Therefore, DAP can be an attractive policy, especially for a large system in which the travel time from the farthest aisle to the workstation is much longer than other aisles. The system is more sensitive to the number of robots and the robot-to-aisle ratio than to the value of the maximum allowed number of robots working in the aisle at the same time (O_b). The optimal height-to-length ratio of the rack is around two for both blocking policies.

With the development of technology, it is possible to track the position of robots at all times. Our policies to handle blocking may be improved by taking these exact robot positions into account. The handling of robot blocking and congestion by considering robot positions and outstanding jobs is a still largely unexplored area. Also, the robots in the CRSR system have the ability to choose different routing trajectories. Therefore, in the future, it will be interesting to study robot routing trajectories, as this may impact the system design and performance. Furthermore, it may be interesting to investigate different dwell points of the robots.

Acknowledgment

The authors thank the editors and anonymous reviewers for constructive comments.

References

Ang M, Lim YF (2019) How to optimize storage classes in a unit-load ware- house. *Eur. J. Oper. Res.* 278(1):186–201.

Ang M, Lim YF, Sim M (2012) Robust storage assignment in unit-load ware- houses. *Management Sci.* 58(11):2114–2130.

Attabotics (2020a) Supply chain presentation. Accessed November 2, 2020, https://www.youtube.com/watch?v=JFPL3Qg4LL0.

Attabotics (2020b) Calgary company reinvents supply chain management. Accessed October 19, 2020, https://www.youtube.com/watch?v=tw8YfIKgblo.

Azadeh K, Roy D, De Koster R (2019a) Design, modeling, and analysis of vertical robotic storage and retrieval systems. *Transportation Sci.* 53(5):1213–1234.

Azadeh K, Roy D, De Koster R (2019b) Robotized and automated warehouse systems: Review and recent developments. *Transportation Sci.* 53(4):917–945.

Balsamo S, De Nitto Persone V, Onvural R (2001) Analysis of queueing networks with blocking. *International Series in Operations Research and Management Science*, vol. 31 (Kluwer Academic Publishers, Boston).

Cai X, Heragu SS, Liu Y (2014) Modeling and evaluating the AVS/RS with tier-to-tier vehicles using a semi-open queueing network. *IIE Trans.* 46(9):905–927.

Ekren BY, Heragu SS, Krishnamurthy A, Malmborg CJ (2014) Matrix-geometric solution for semi-open queuing network model of autonomous vehicle storage and retrieval system. *Comput. Indust. Engrg.* 68(February):78–86.

Epp M, Wiedemann S, Furmans K (2016) A discrete-time queueing network approach to performance evaluation of autonomous vehicle storage and retrieval systems. *Internat. J. Production Res.* 55(3):960–978.

Exotec (2020a) Exotec. Accessed March 11, 2020, https://www.youtube.com/watch? v=WR2Oufh80T8.

Exotec (2020b) Exotec. Our products. Skypod System: The 3rd dimension of your supply chain. Accessed April 27, 2020, https://www.youtube.com/watch?v=IRwyOPO6KR4.

Exotec Solutions (2019) Elegant warehouse robotics for a volatile world. Accessed July 7, 2019, http://www.exotecsolutions.com/.

Flexsim (2019) The 3D simulation modeling and analysis software. Accessed March 18, 2019, http://www.flexsim.com/.

Fukunari M, Malmborg CJ (2008) An efficient cycle time model for autonomous vehicle storage and retrieval systems. *Internat. J. Production Res.* 46(12):3167–3184.

Gue KR, Kim BS (2007) Puzzle-based storage systems. *Naval Res. Logist.* 54(5):556–567.

Heragu SS, Cai X, Krishnamurthy A, Malmborg CJ (2011) Analytical models for analysis of automated warehouse material handling systems. *Internat. J. Production Res.* 49(22):6833–6861.

Kuo PH, Krishnamurthy A, Malmborg CJ (2007) Design models for unit load storage and retrieval systems using autonomous vehicle technology and resource conserving storage and dwell point policies. *Appl. Math. Model.* 31(10):2332–2346.

Lamballais T, Roy D, De Koster R (2020) Inventory allocation in robotic mobile fulfillment systems. *IISE Trans.* 52(1):1–17.

Malmborg CJ (2002) Conceptualizing tools for autonomous vehicle storage and retrieval systems. *Internat. J. Production Res.* 40(8):1807–1822.

Marchet G, Melacini M, Perotti S, Tappia E (2012) Analytical model to estimate performances of autonomous vehicle storage and retrieval systems for product totes. *Internat. J. Production Res.* 50(24):7134–7148.

Merschformann M, Lamballais T, De Koster R, Suhl L (2019) Decision rules for robotic mobile fulfillment systems. *Oper. Res. Perspect.* 6(November):100128–100143.

Papadopoulos HT, Heavey C (1996) Queueing theory in manufacturing systems analysis and design: A classification of models for production and transfer lines. *Eur. J. Oper. Res.* 92(1):1–27.

Perros H (1994) *Queueing Networks with Blocking: Exact and Approximate Solutions* (Oxford University Press, New York).

Roy D, Krishnamurthy A, Heragu SS, Malmborg CJ (2012) Performance analysis and design trade-offs in warehouses with autonomous vehicle technology. *IIE Trans.* 44(12):1045–1060.

Roy D, Krishnamurthy A, Heragu SS, Malmborg CJ (2014) Blocking effects in warehouse systems with autonomous vehicles. *IEEE Trans. Automation Sci. Engrg.* 11(2):439–451.

Roy D, Krishnamurthy A, Heragu SS, Malmborg CJ (2015) Queuing models to analyze dwell-point and cross-aisle location in

autonomous vehicle-based warehouse systems. *Eur. J. Oper. Res.* 242(1):72–87.

Roy D, Krishnamurthy A, Heragu SS, Malmborg CJ (2016) A simulation framework for studying blocking effects in warehouse systems with autonomous vehicles. *Eur. J. Indust. Engrg.* 10(1): 51–80.

Roy D, Krishnamurthy A, Heragu SS, Malmborg CJ (2017) A multi-tier linking approach to analyze performance of autonomous vehicle-based storage and retrieval systems. *Comput. Oper. Res.* 83(July):173–188.

Roy D, Nigam S, De Koster R, Adan IRJ (2019) Robot-storage zone assignment strategies in mobile fulfillment systems. *Transportation Res. Part E Logist. Transportation Rev.* 122(1): 119–142.

Tappia E, Roy D, De Koster R, Melacini M (2016) Modeling, analysis, and design insights for shuttle-based compact storage systems. *Transportation Sci.* 51(1):269–295.

Tappia E, Roy D, Melacini M, De Koster R (2019) Integrated storage-order picking systems: Technology, performance models, and design insights. *Eur. J. Oper. Res.* 274(3):947–965.

Van der Gaast JP, De Koster R, Adan IJBF, Resing JAC (2020) Capacity analysis of sequential zone picking systems. *Oper. Res.* 68(1):161–179.

Van Dijk NM (1988) On Jackson's product form with jump-over-blocking. *Oper. Res. Lett.* 7(5):233–235.

Weidinger F, Boysen N, Briskorn D (2018) Storage assignment with rack-moving mobile robots in KIVA warehouses. *Transportation Sci.* 52(6):1479–1495.

Yao DD, Buzacott JA (1987) Modeling a class of flexible manufacturing systems with reversible routing. *Oper. Res.* 35(1):87–93.

Yu Y, De Koster R, Guo X (2015) Class-based storage with a finite number of items: Using more classes is not always better. *Production Oper. Management* 24(8):1235–1247.

Yuan Z, Gong Y (2017) Bot-in-time delivery for robotic mobile fulfillment systems. *IEEE Trans. Eng. Management* 64(1):83–93.

Zaerpour N, Yu Y, De Koster R (2017a) Response time analysis of a live-cube compact storage system with two storage classes. *IISE Trans.* 49(5):461–480.

Zaerpour N, Yu Y, De Koster R (2017b) Small is beautiful: A framework for evaluating and optimizing live-cube compact storage systems. *Transportation Sci.* 51(1):34–51.

Zou B, Gong Y, Xu X, Yuan Z (2017) Assignment rules in robotic mobile fulfilment systems for online retailers. *Internat. J. Production Res.* 55(20):6175–6192.

Zou B, Xu X, Gong Y, De Koster R (2016) Modeling parallel movement of lifts and vehicles in tier-captive vehicle-based warehousing systems. *Eur. J. Oper. Res.* 254(1):51–67.

Zou B, Xu X, Gong Y, De Koster R (2018) Evaluating battery charging and swapping strategies in a robotic mobile fulfllment system. *Eur. J. Oper. Res.* 267(2):733–753.